

Spindle orientation in *Saccharomyces cerevisiae* depends on the transport of microtubule ends along polarized actin cables

Eric Hwang,¹ Justine Kusch,² Yves Barral,² and Tim C. Huffaker¹

¹Department of Molecular Biology and Genetics, Cornell University, Ithaca, NY 14853

²Swiss Federal Institute of Technology (ETH), Institute of Biochemistry, CH-8093 Zürich, Switzerland

Microtubules and actin filaments interact and cooperate in many processes in eukaryotic cells, but the functional implications of such interactions are not well understood. In the yeast *Saccharomyces cerevisiae*, both cytoplasmic microtubules and actin filaments are needed for spindle orientation. In addition, this process requires the type V myosin protein Myo2, the microtubule end-binding protein Bim1, and Kar9. Here, we show that fusing Bim1 to the tail of the Myo2 is sufficient to orient spindles in the absence of Kar9, suggesting that the role of

Kar9 is to link Myo2 to Bim1. In addition, we show that Myo2 localizes to the plus ends of cytoplasmic microtubules, and that the rate of movement of these cytoplasmic microtubules to the bud neck depends on the intrinsic velocity of Myo2 along actin filaments. These results support a model for spindle orientation in which a Myo2–Kar9–Bim1 complex transports microtubule ends along polarized actin cables. We also present data suggesting that a similar process plays a role in orienting cytoplasmic microtubules in mating yeast cells.

Introduction

Microtubules and actin filaments are known to cooperate in a variety of processes in diverse cell types, but the molecular mechanisms underlying these interactions are not well understood (Goode et al., 2000). One of these processes is spindle orientation in the budding yeast *Saccharomyces cerevisiae*. Orientation of the yeast preanaphase spindle at the bud neck is necessary to ensure that subsequent spindle elongation delivers chromosomes to both the mother and daughter cells. Spindle orientation depends on cytoplasmic microtubules that originate from the spindle pole bodies (Palmer et al., 1992; Sullivan and Huffaker, 1992) and on a polarized array of actin cables that focus toward the bud (Palmer et al., 1992; Theesfeld et al., 1999). It also depends on the unconventional myosin Myo2 (Beach et al., 2000; Yin et al., 2000), the microtubule-binding protein Bim1 (Schwartz et al., 1997; Tirnauer and Bierer, 2000), and Kar9 (Miller and Rose, 1998). The discovery that Kar9 interacts with Myo2 (Yin et al., 2000) and Bim1 (Korinek et al.,

2000; Lee et al., 2000; Miller et al., 2000) led to two alternative models to explain the roles of actin filaments and microtubules in spindle orientation. First, Kar9 might be transported by Myo2 along actin filaments into the bud. Once stabilized in the bud, Kar9 could then serve as a capture site for probing dynamic Bim1-coated microtubule ends (Bloom, 2000) in accord with the general principles proposed by Kirschner and Mitchison (1986). Alternatively, Kar9 might cross-bridge Myo2 and Bim1 so that the movement of Myo2 along actin filaments could actively pull microtubule ends toward the bud (Yin et al., 2000). These models differ in the fundamental mechanism by which microtubules are oriented, either a stochastic or a directed process. Here, we provide evidence that supports the latter model.

Results and discussion

A Myo2–Bim1 fusion is sufficient to orient spindles in the absence of Kar9

If the role of Kar9 is to cross-bridge Myo2 and Bim1, we reasoned that Kar9 would not be required if Bim1 was fused directly to the tail of Myo2. To test this idea, we integrated the *BIM1* coding sequence downstream of the chromosomal *MYO2* coding sequence to create a *MYO2–BIM1* fusion in cells lacking Kar9 (*kar9Δ*). Myo2–Bim1 is the only source of Myo2 function in these cells, and it is

The online version of this article includes supplemental material.

Address correspondence to Tim Huffaker, Dept. of Molecular Biology and Genetics, Biotechnology Building, Cornell University, Ithaca, NY 14853-2703. Tel.: (607) 255-9947. Fax: (607) 255-6249. E-mail: tch4@cornell.edu

Key words: cytoskeleton; microfilaments; microtubules; mitotic spindle apparatus; myosins

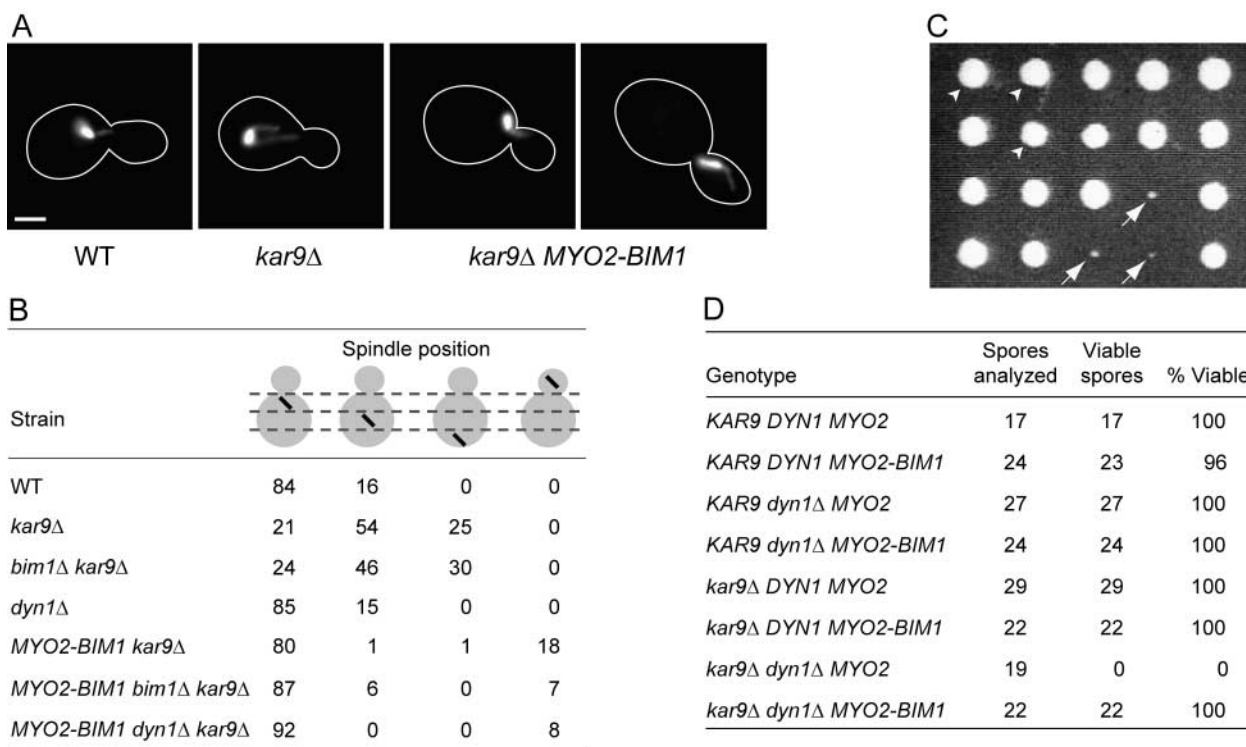


Figure 1. **MYO2-BIM1 fusion compensates for the spindle orientation defect in *kar9Δ* cells.** (A and B) Microtubule immunofluorescence was used to determine the localization of preanaphase spindles. (A) Examples of spindle localization in wild-type, *kar9Δ*, and *kar9Δ MYO2-BIM1* cells. Bar, 2 μ m. (B) The percentage of cells with spindles located in each of four different regions of budded cells. (C and D) A *MYO2-BIM1::URA3 kar9Δ::LEU2* strain was crossed to a *dyn1Δ::HIS3* strain. The resulting diploid was sporulated, and 46 tetrads were dissected. The genotype of meiotic segregants was determined by scoring for the linked auxotrophic markers. The genotype of inviable spores could be inferred in all cases by assuming 2:2 segregation of markers. (C) Growth of meiotic segregants from five tetrads. *kar9Δ dyn1Δ* strains (indicated by arrows) formed microcolonies that did not grow further. *kar9Δ dyn1Δ MYO2-BIM1* strains (indicated by arrowheads) were viable, and grew as well as wild-type cells. (D) Viability of spores of each genotype obtained from the cross.

expressed from the endogenous *MYO2* promoter. Although *MYO2* is an essential gene (Johnston et al., 1991), replacing endogenous *MYO2* with *MYO2-BIM1* did not have any deleterious effect on the growth rate of the cells. In fact, the presence of *MYO2-BIM1* slightly increased the growth rate of *kar9Δ* cells. The doubling times for *MYO2 KAR9*, *MYO2 kar9Δ*, and *MYO2-BIM1 kar9Δ* cells are 90, 100, and 90 min, respectively, in rich medium at 30°C.

We measured the ability of Myo2-Bim1 to replace Kar9 in two ways. First, we examined the location of preanaphase spindles by fluorescence microscopy (Fig. 1, A and B). In wild-type cells, most preanaphase spindles are located adjacent to the bud neck. As expected, *kar9Δ* cells showed a marked defect in orienting spindles at the bud neck (Miller and Rose, 1998). Myo2-Bim1 completely compensated for loss of Kar9. Spindle orientation also occurs efficiently in *MYO2-BIM1 kar9Δ bim1Δ* cells, indicating that neither Myo2, Kar9, nor Bim1 is needed if cells express Myo2-Bim1. In a portion of the *MYO2-BIM1 kar9Δ* cells, the preanaphase spindle was located entirely within the bud. This latter phenotype agrees with the recently described role of Kar9 in ensuring that only one spindle pole migrates to the bud (Liakopoulos et al., 2003), a role that is not provided by Myo2-Bim1.

We also used a genetic test to assay whether Myo2-Bim1 can replace Kar9. *KAR9* is not an essential gene, but cells

lacking both *KAR9* and the gene encoding dynein heavy chain, *DYN1*, are inviable (Miller and Rose, 1998). Dynein is not required for preanaphase spindle orientation (Fig. 1 B), but can compensate for the loss of Kar9 as it plays a role in movement of the spindle through the bud neck during anaphase (Yeh et al., 1995; Carminati and Stearns, 1997). Because loss of *DYN1* makes *KAR9* essential for viability, we asked whether *MYO2-BIM1* could complement the lethality of *kar9Δ dyn1Δ* mutants. We crossed a *MYO2-BIM1 kar9Δ* strain to a *dyn1Δ* strain and analyzed the genotype of meiotic segregants (Fig. 1, C and D). As expected, all *kar9Δ dyn1Δ* spores produced microcolonies of cells that were inviable. However, *MYO2-BIM1 kar9Δ dyn1Δ* strains were viable, and grew as well as wild-type cells (90-min doubling time in rich medium at 30°C). In addition, these cells did not exhibit any defect in preanaphase spindle orientation (Fig. 1 B).

A Myo2-Bim1 fusion is sufficient to orient cytoplasmic microtubules in mating yeast cells in the absence of Kar9

A motile process similar to spindle orientation occurs during yeast mating. When yeast cells sense mating factors secreted by cells of the opposite mating type, they form a mating projection. Cytoplasmic microtubules extend toward the tip of this projection and mediate the migration of the nucleus into it (Maddox et al., 1999). Actin is also required for mi-

gration of the nucleus into the mating projection (Read et al., 1992), suggesting that the mechanism may be similar to that used for spindle orientation. Both *kar9Δ* and *bim1Δ* mutants display defects in karyogamy during mating because they fail to orient microtubules correctly (Schwartz et al., 1997; Miller and Rose, 1998).

We wanted to determine whether Myo2 also plays a role in this process. Myo2 contains an amino-terminal motor domain and a carboxy-terminal tail domain that binds cargo. A series of temperature-sensitive *myo2* tail domain mutants have been described that inhibit polarized localization of secretory vesicles at their restrictive temperature (Schott et al., 1999). In this work, we used three of these alleles, *myo2-17* that has little effect on spindle orientation and *myo2-18* and *myo2-20* that have more significant effects on spindle orientation (Yin et al., 2000).

MATa cells were exposed to the mating pheromone α -factor, causing them to arrest as unbudded cells with an elongated mating projection. After α -factor arrest, wild-type and *myo2* mutant cells were shifted to 35°C for 5 min, and microtubule orientation was assayed (Fig. 2, A and B). The temperature shift had no effect on microtubule orientation in wild-type cells, whereas *myo2* mutant cells showed a marked decrease in microtubule orientation at the restrictive temperature. As was the case for spindle orientation, this phenotype was most apparent in the *myo2-18* and *myo2-20* mutants. The rapid effect of the *myo2* mutations suggests a direct role for the tail of Myo2 in this process.

Next, we tested the ability of Myo2–Bim1 to substitute for Kar9 in α -factor-treated cells. As shown previously (Miller and Rose, 1998), loss of Kar9 had a severe effect on the orientation of microtubules to the tip of the mating projection (Fig. 2 C). Introduction of *MYO2–BIM1* into *kar9Δ* cells restored microtubule orientation to wild-type levels. These results indicate that the mechanisms of microtubule orientation are similar in mitotic and mating cells.

The rate of cytoplasmic microtubule tip movement depends on the intrinsic velocity of Myo2

We have shown that fusing the microtubule-binding protein Bim1 to the tail of the actin motor Myo2 eliminates the requirement for Kar9 in growing and mating yeast cells, suggesting that the cellular role of Kar9 is to cross-bridge Myo2 and Bim1. This result supports the model in which a Myo2–Kar9–Bim1 complex transports microtubule ends along polarized actin cables. To test this model directly, we used a slow-moving variant of Myo2. The rate at which Myo2 moves is influenced by the length of its lever arm. The wild-type Myo2 lever arm has six IQ repeats, and variants have been made that lack some or all of these IQ repeats. These mutants have been used to demonstrate that secretory vesicle movement in yeast depends on Myo2, and define a linear relationship between the number of IQ repeats in Myo2 and the rate of vesicle movement (Stevens and Davis, 1998; Schott et al., 2002).

We used cells expressing GFP–Tub1 to measure the rate of cytoplasmic microtubule tip movement in strains containing either zero or six IQ repeat Myo2 as their sole source of the Myo2. In budded cells, cytoplasmic microtubules em-

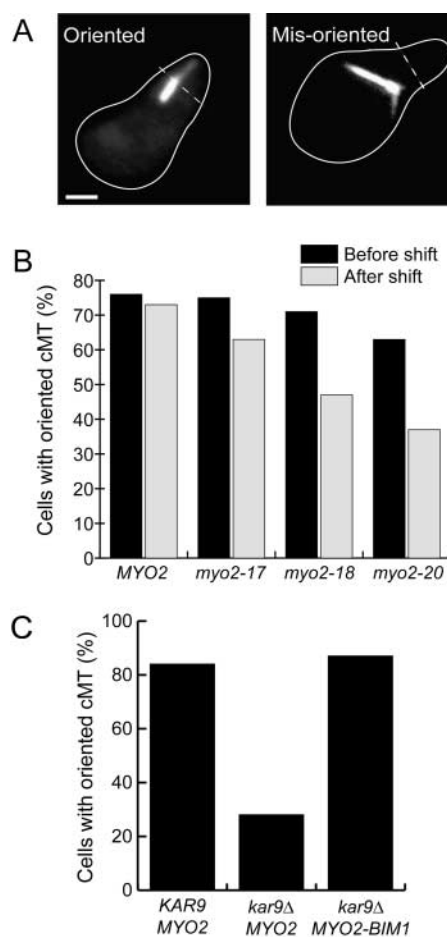


Figure 2. MYO2–BIM1 fusion compensates for the microtubule orientation defect in α -factor-treated *kar9Δ* cells. (A) Examples of an oriented microtubule that extends into the mating projection tip and a misoriented microtubule that does not extend into the projection tip of α -factor-treated cells. The projection tip (indicated by the dotted line) was defined by drawing a line perpendicular to the long axis of the cell and one quarter of the cell's length away from the end of the projection. Microtubules were visualized by immunofluorescence microscopy. Bar, 2 μ m. (B) The percentage of *MYO2* and conditional *myo2* mutant yeast cells with microtubules oriented toward the projection tip was determined before (black bars) and after a 5-min shift to the restrictive temperature of 35°C (gray bars). 100 cells were counted in each case. (C) The percentage of wild-type, *KAR9MYO2*, and *kar9Δ MYO2* cells with microtubules oriented toward the projection tip. 50 cells were counted in each case.

anating from the bud-proximal spindle pole commonly extend to the edge of the mother cell, and then move toward the bud neck (Liakopoulos et al., 2003). In wild-type cells, this movement occurs within a couple of seconds and without any significant change in microtubule length. Strikingly, the velocities of these movements depend on the number of IQ repeats in Myo2 (Fig. 3 and Videos 1 and 2, available at <http://www.jcb.org/cgi/content/full/jcb.200302030/DC1>). The average rate of microtubule movement is nearly five times slower in cells containing the Myo2 that lacks IQ repeats (1.22 ± 0.36 vs. 0.26 ± 0.09 μ m/s). These results unambiguously demonstrate that Myo2 directs the movement of microtubule tips.

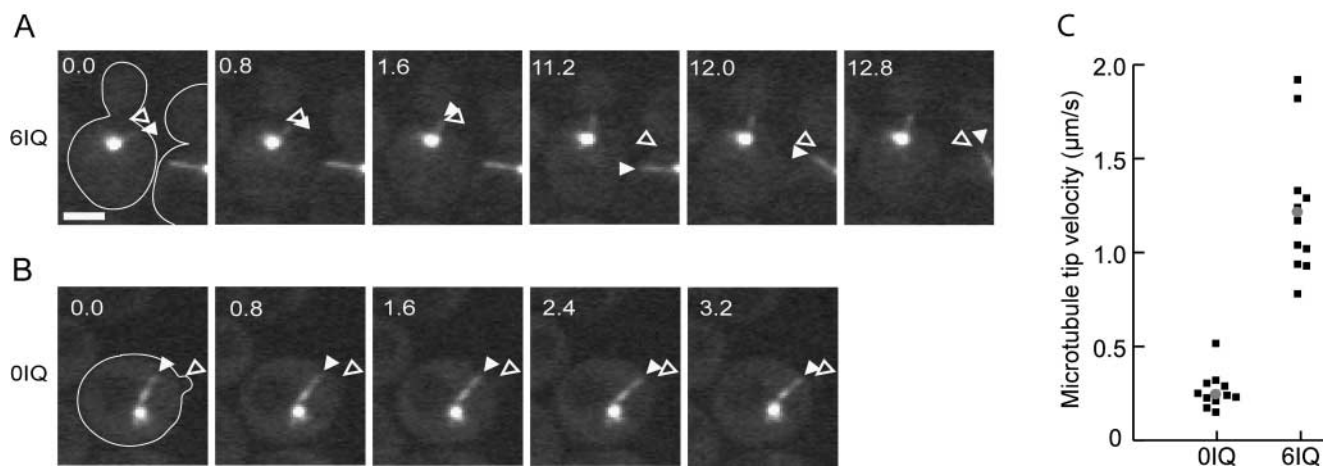


Figure 3. The rate of cytoplasmic microtubule movement depends of the intrinsic velocity of Myo2. (A and B) Fluorescence images of live cells containing GFP–Tub1. Time intervals (in seconds) between images are indicated in the top left of each image. White arrowhead tracks movement of microtubule end; open arrowhead is a fiduciary marker near the bud neck. Bar, 2 μm . (A) Cells containing wild-type Myo2 with six IQ repeats. Microtubule in cell on left begins movement at 0.0 s; microtubule in cell on right begins movement at 11.2 s (see Video 1). (B) Cell containing a mutant Myo2 lacking IQ repeats (see Video 2). (C) Scatter plot of cytoplasmic microtubule tip velocities. Each black square corresponds to an individual measurement (11 measurements for 0 IQ and 12 for 6 IQ). Gray dots indicate average velocities.

Myo2 is associated with the tips of cytoplasmic microtubules

The observation that microtubules orient toward the bud neck in a Myo2-dependent manner suggested that Myo2 associates with microtubule ends in the mother cell. Given that Myo2 is a prominent protein involved in a variety of cellular processes, we would expect only a tiny portion of the cellular Myo2 to be associated with microtubule ends. Initially, we visualized Myo2–Bim1 by immunofluorescence microscopy using an antibody directed against Myo2 (Fig. 4 A). The localization of Myo2–Bim1 is similar to that for Myo2 in wild-type cells (Lillie and Brown, 1994). The protein is concentrated in the bud, particularly at the bud tip, but a weaker staining is also observed in the mother cell. We did not notice specific localization of Myo2–Bim1 with the tips of cytoplasmic microtubules. However, the long fixation time needed to preserve cytoplasmic microtubules for immunofluorescence could make it difficult to observe transient interactions.

Next, we attempted to visualize interactions between Myo2 and microtubules in live cells. In cells expressing CFP–Tub1, Myo2 was replaced by a fully functional Myo2–GFP fusion protein. In about a quarter of the cells, GFP dots labeled the plus end of microtubules (Fig. 4 B). Such staining was not restricted to the bud, where most of the Myo2 localizes, but was also observed in the mother compartment. In cells with an oriented short spindle, Myo2–GFP was observed only on microtubules coming from the bud-proximal pole (unpublished data). This experiment likely underestimates the fraction of microtubule ends that associate with Myo2. Imaging CFP–Tub1 requires relatively long exposure times (1–2 s) making it difficult to catch colocalization events. Therefore, we also compared fluorescence images of cells expressing GFP–Tub1 with cells coexpressing GFP–Tub1 and Myo2–GFP in an attempt to see whether the presence of Myo2–GFP modified the GFP staining observed in cells expressing GFP–Tub1 alone. Our

rationale was that if Myo2–GFP accumulated at the tip of microtubules, then this should be reflected by an increased fluorescence intensity at this location. Because the Myo2 and Tub1 signals are acquired more rapidly and simultaneously in the same channel, colocalization should be easier to observe with this approach. Comparison of GFP–Tub1 alone with GFP–Tub1 Myo2–GFP indicates that a stronger dot appears at the tip of virtually all microtubules in the presence of Myo2–GFP specifically (Fig. 4, C and D). This signal was observed even on microtubules that had not yet reached the bud compartment.

To test whether this observation was significant, images of microtubules were collected and the intensity of the GFP signal along the microtubules was analyzed statistically, starting from the plus end. This analysis was restricted to microtubules that had not reached the bud neck or the bud to minimize artifacts due to the general localization of Myo2. Our analysis focused on microtubules emanating from the pole proximal to the bud. This work indicated an increase in intensity at microtubule plus ends that was highly reproducible and due to Myo2–GFP because it was not observed if Myo2 was not tagged (Fig. 4 E). Interestingly, it was no longer observed in cells lacking Kar9, consistent with the idea that Kar9 is required to recruit Myo2 onto microtubules. The same analysis failed to show Myo2 staining on microtubules coming from the mother-bound pole (unpublished data). Thus, our results indicate that Myo2 localizes in a Kar9-dependent manner to the plus ends of microtubules coming from the daughter-bound pole. This recruitment of Myo2 to specific microtubules may determine which microtubules orient toward the bud.

In summary, our results support a model in which a Myo2–Kar9–Bim1 complex transports microtubule ends along polarized actin cables (Fig. 5). Whether this process provides a motive force for orienting spindles or simply orients cytoplasmic microtubules that subsequently act to provide force (Kusch et al., 2002) remains to be elucidated. Co-

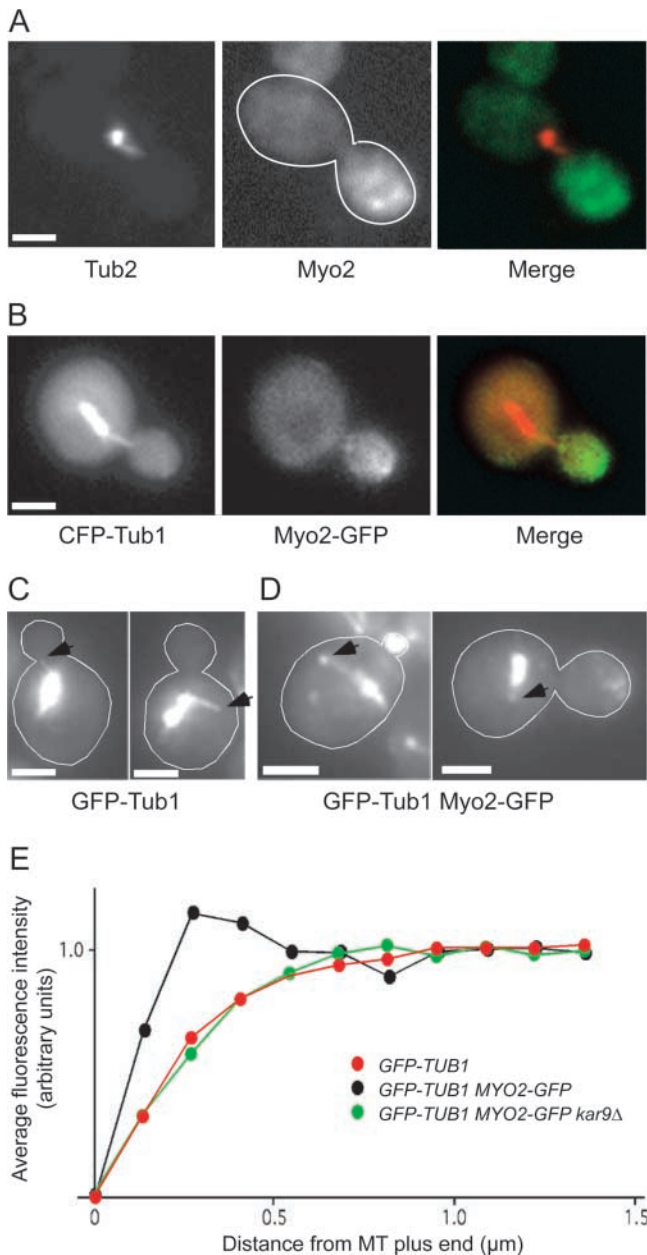


Figure 4. Myo2 is associated with the tips of cytoplasmic microtubules. (A) Immunofluorescence microscopy of *MYO2-BIM1* cells using anti-Tub2 and anti-Myo2 antibodies. (B–D) Fluorescence images of live cells containing (B) CFP-Tub1 and Myo2-GFP, (C) GFP-Tub1, and (D) GFP-Tub1 and Myo2-GFP. (E) Plot of average fluorescence intensities along cytoplasmic microtubules, starting from just off the plus ends, in *GFP-TUB1* cells, *GFP-TUB1 MYO2-GFP* cells, and *GFP-TUB1 MYO2-GFP kar9Δ* cells. Intensities along 20 microtubules were measured for each cell type. Bars, 2 μm.

ordination of the orientation of the mitotic spindle with actin-based cortical structures has been observed in several systems, and may require the Bim1 homologue, EBI, that is found at microtubule ends (Rose and Kemphues, 1998; Bizenz, 2001). In addition, microtubules in interphase cells have been reported to target to focal adhesions, although the molecular mechanisms remain elusive (Tepass et al., 2001). Based on the model supported here, we suspect that the mechanisms might include directed delivery of microtubule

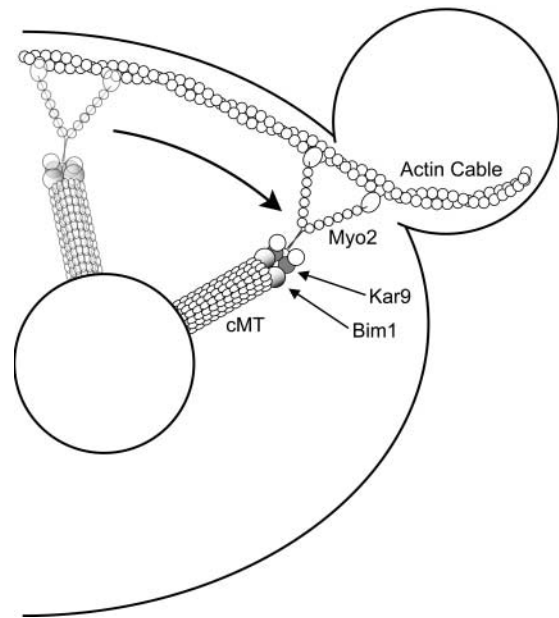


Figure 5. Model for cytoplasmic microtubule orientation in budding yeast. Cytoplasmic microtubules arise from the spindle pole body and extend toward the mother cell cortex. Kar9 interacts with the microtubule end-binding protein Bim1, and with the tail of Myo2. Movement of Myo2 along polarized actin filaments transports the end of the microtubule to the bud neck. Further myosin-dependent movement or microtubule shortening could then serve to draw the spindle toward the bud.

ends by myosin motors transporting along polarized actin filaments.

Materials and methods

Yeast strains and plasmids

Yeast strains carrying temperature-sensitive *myo2* alleles (Schott et al., 1999), the *myo2* allele lacking IQ repeats (Stevens and Davis, 1998), *kar9Δ* (Miller and Rose, 1998), *dyn1Δ* (Eshel et al., 1993; Li et al., 1993) and *bim1Δ* (Schwartz et al., 1997) deletions, and GFP-Tub1 (Kosco et al., 2001) and CFP-Tub1 (Kusch et al., 2002) have been described previously.

A strain containing *MYO2-BIM1::URA3* was constructed using the one-step PCR method for gene modification (Longtine et al., 1998) to integrate the coding sequence for *BIM1* just downstream of the chromosomal *MYO2* coding sequence. Thus, *MYO2-BIM1* encodes full-length Myo2 followed by a short linker polypeptide (Ala-Gly-Ala-Gly-Ala), followed by full-length Bim1. *MYO2-BIM1* was initially created in the diploid strain CUY1415 (*MATa/MATα kar9Δ::LEU2/kar9Δ::LEU2 his3-Δ200/his3-Δ200 leu2-3,112/leu2-3,112 lys2-801/lys2-801 ura3-52/ura3-52*). Sporulation and tetrad dissection yielded a haploid strain CUY1408 (*MATa MYO2-BIM1::URA3 kar9Δ::LEU2 his3-Δ200 leu2-3,112 lys2-801 ura3-52*). *MYO2-BIM1* is the only source of *MYO2* function in these cells, and it is expressed from the endogenous *MYO2* promoter.

A strain containing *MYO2-GFP::kanMX* was also constructed using the one-step PCR method for gene modification. *MYO2-GFP* encodes full-length Myo2 followed directly by GFP. This protein fusion is also expressed from the endogenous *MYO2* promoter.

Fluorescence microscopy

Visualization of microtubules by immunofluorescence microscopy was performed as described previously (Pasqualone and Huffaker, 1994). Visualization of GFP- and CFP-conjugated proteins was done in live cells. Single images were collected under a conventional fluorescence microscope with a 100× objective and a CCD detector using Openlab (Improvision) or TILLVISION (T.I.L.L. Photonics) software (Kusch et al., 2002). Time-lapse images of cytoplasmic microtubule movement were collected at 0.2- or 0.4-s intervals using a live cell imaging system (UltraVIEW™; PerkinElmer).

Online supplemental material

Video 1 shows cytoplasmic microtubule movement in cells containing GFP-Tub1 and wild-type Myo2 with six IQ repeats. Video 2 shows cytoplasmic microtubule movement in cells containing GFP-Tub1 and a mutant Myo2 lacking IQ repeats. Online supplemental material available at <http://www.jcb.org/cgi/content/full/jcb.200302030/DC1>.

We thank Tony Bretscher, Hongwei Yin, Daniel Schott, and David Pruyne for reagents and helpful discussions; Bill Brown and Tony Bretscher for use of their microscope; and Bret Judson for help with microscopy.

This work was supported by grants from the National Institutes of Health to T.C. Huffaker (GM40479) and from the Swiss Federal Institute of Technology (ETH) to Y. Barral and J. Kusch. Y. Barral is a member of the EMBO young investigator program.

Submitted: 5 February 2003

Revised: 26 March 2003

Accepted: 26 March 2003

References

- Beach, D.L., J. Thibodeaux, P. Maddox, E. Yeh, and K. Bloom. 2000. The role of the proteins Kar9 and Myo2 in orienting the mitotic spindle of budding yeast. *Curr. Biol.* 10:1497–1506.
- Bienz, M. 2001. Spindles cotton on to junctions, APC and EB1. *Nat. Cell Biol.* 3:E67–E68.
- Bloom, K. 2000. It's a kar9ochore to capture microtubules. *Nat. Cell Biol.* 2:E96–E98.
- Carminati, J.L., and T. Stearns. 1997. Microtubules orient the spindle in yeast through dynein-dependent interactions with the cell cortex. *J. Cell Biol.* 138:629–642.
- Eshel, D., L.A. Urrestarazu, S. Vissers, J.-C. Jauniaux, J.C. van Vleit-Reedijk, R.J. Planta, and I.R. Gibbons. 1993. Cytoplasmic dynein is required for normal nuclear segregation in yeast. *Proc. Natl. Acad. Sci. USA.* 90:11172–11176.
- Goode, B.L., D.G. Drubin, and G. Barnes. 2000. Functional cooperation between the microtubule and actin cytoskeletons. *Curr. Opin. Cell Biol.* 12:63–71.
- Johnston, G., J. Prendergast, and R. Singer. 1991. The *Saccharomyces cerevisiae* *MYO2* gene encodes an essential myosin for vectorial transport of vesicles. *J. Cell Biol.* 113:539–551.
- Kirschner, M., and T. Mitchison. 1986. Beyond self-assembly: from microtubules to morphogenesis. *Cell.* 45:329–342.
- Korinek, W.S., M.J. Copeland, A. Chaudhuri, and J. Chant. 2000. Molecular linkage underlying microtubule orientation toward cortical sites in yeast. *Science.* 287:2257–2259.
- Kosco, K.A., C.G. Pearson, P.S. Maddox, P.J. Wang, I.R. Adams, E.D. Salmon, K. Bloom, and T.C. Huffaker. 2001. Control of microtubule dynamics by stu2p is essential for spindle orientation and metaphase chromosome alignment in yeast. *Mol. Biol. Cell.* 12:2870–2880.
- Kusch, J., A. Meyer, M.P. Snyder, and Y. Barral. 2002. Microtubule capture by the cleavage apparatus is required for proper spindle positioning in yeast. *Genes Dev.* 16:1627–1639.
- Lee, L., J.S. Tirnauer, J. Li, S.C. Schuyler, J.Y. Liu, and D. Pellman. 2000. Positioning of the mitotic spindle by a cortical-microtubule capture mechanism. *Science.* 287:2260–2262.
- Li, Y.Y., E. Yeh, T. Hays, and K. Bloom. 1993. Disruption of mitotic spindle orientation in a yeast dynein mutant. *Proc. Natl. Acad. Sci. USA.* 90:10096–10100.
- Liakopoulos, D., J. Kusch, S. Grava, J. Vogel, and Y. Barral. 2003. Asymmetric loading of Kar9 onto spindle poles and microtubules ensures proper spindle alignment. *Cell.* 112:561–574.
- Lillie, S.H., and S.S. Brown. 1994. Immunofluorescence localization of the unconventional myosin, Myo2p, and the putative kinesin-related protein, Smy1p, to the same regions of polarized growth in *Saccharomyces cerevisiae*. *J. Cell Biol.* 125:825–842.
- Longtine, M.S., A. McKenzie 3rd, D.J. Demarini, N.G. Shah, A. Wach, A. Brachat, P. Philippsen, and J.R. Pringle. 1998. Additional modules for versatile and economical PCR-based gene deletion and modification in *Saccharomyces cerevisiae*. *Yeast.* 14:953–961.
- Maddox, P., E. Chin, A. Mallavarapu, E. Yeh, E.D. Salmon, and K. Bloom. 1999. Microtubule dynamics from mating through the first zygotic division in the budding yeast *Saccharomyces cerevisiae*. *J. Cell Biol.* 144:977–987.
- Miller, R.K., and M.D. Rose. 1998. Kar9p is a novel cortical protein required for cytoplasmic microtubule orientation in yeast. *J. Cell Biol.* 140:377–390.
- Miller, R.K., S.C. Cheng, and M.D. Rose. 2000. Bim1p/Yeb1p mediates the Kar9p-dependent cortical attachment of cytoplasmic microtubules. *Mol. Biol. Cell.* 11:2949–2959.
- Palmer, R.E., D.S. Sullivan, T. Huffaker, and D. Koshland. 1992. Role of astral microtubules and actin in spindle orientation and migration in the budding yeast, *Saccharomyces cerevisiae*. *J. Cell Biol.* 119:583–593.
- Pasqualone, D., and T.C. Huffaker. 1994. *STU1*, a suppressor of a β -tubulin mutation, encodes a novel and essential component of the yeast mitotic spindle. *J. Cell Biol.* 127:1973–1984.
- Read, E.B., H.H. Okamura, and D.G. Drubin. 1992. Actin- and tubulin-dependent functions during *Saccharomyces cerevisiae* mating projection formation. *Mol. Biol. Cell.* 3:429–444.
- Rose, L.S., and K.J. Kemphues. 1998. Early patterning of the *C. elegans* embryo. *Annu. Rev. Genet.* 32:521–545.
- Schott, D., J. Ho, D. Pruyne, and A. Bretscher. 1999. The COOH-terminal domain of Myo2p, a yeast myosin V, has a direct role in secretory vesicle targeting. *J. Cell Biol.* 147:791–808.
- Schott, D.H., R.N. Collins, and A. Bretscher. 2002. Secretory vesicle transport velocity in living cells depends on the myosin-V lever arm length. *J. Cell Biol.* 156:35–39.
- Schwartz, K., K. Richards, and D. Botstein. 1997. *BIM1* encodes a microtubule-binding protein in yeast. *Mol. Biol. Cell.* 8:2677–2691.
- Stevens, R.C., and T.N. Davis. 1998. Mlc1p is a light chain for the unconventional myosin Myo2p in *Saccharomyces cerevisiae*. *J. Cell Biol.* 142:711–722.
- Sullivan, D.S., and T.C. Huffaker. 1992. Astral microtubules are not required for anaphase B in *Saccharomyces cerevisiae*. *J. Cell Biol.* 119:379–388.
- Tepass, U., G. Tanentzapf, R. Ward, and R. Fehon. 2001. Epithelial cell polarity and cell junctions in *Drosophila*. *Annu. Rev. Genet.* 35:747–784.
- Theesfeld, C.L., J.E. Irazoqui, K. Bloom, and D.J. Lew. 1999. The role of actin in spindle orientation changes during the *Saccharomyces cerevisiae* cell cycle. *J. Cell Biol.* 146:1019–1032.
- Tirnauer, J.S., and B.E. Bierer. 2000. EB1 proteins regulate microtubule dynamics, cell polarity, and chromosome stability. *J. Cell Biol.* 149:761–766.
- Yeh, E., R.V. Skibbens, J.W. Cheng, E.D. Salmon, and K. Bloom. 1995. Spindle dynamics and cell cycle regulation of dynein in the budding yeast, *Saccharomyces cerevisiae*. *J. Cell Biol.* 130:687–700.
- Yin, H., D. Pruyne, T.C. Huffaker, and A. Bretscher. 2000. Myosin V orientates the mitotic spindle in yeast. *Nature.* 406:1013–1015.